A NEW GLOBAL TOPOGRAPHIC MAP OF IO: IMPLICATIONS FOR GLOBAL SHAPE AND INTERNAL HEATING. O.L. White[1] and P.M. Schenk[2]. [1]NASA Ames Research Center, MS 245-3, Moffett Field, CA 94035 (oliver.l.white@nasa.gov), [2]Lunar and Planetary Institute, 3600 Bay Area Boulevard, Houston, TX 77058 (schenk@lpi.usra.edu).

Introduction: No instrumentation specifically designed to measure the topography of a planetary surface has ever been deployed to the Galilean moon Io. Available methods that exist to perform such a task in the absence of the relevant instrumentation include stereo imaging [1], photoclinometry [2], and shadow length measurement [3,4]. In addition, Galileo limb profiles provide the only available global topographic 'ground data' [5].

Stereo-derived digital terrain models (DTMs) are reliable at global and regional scales, but are unable to resolve fine-scale topographic features. Io presents a challenging subject for stereo imaging given that much of its surface is comprised of smooth, low-contrast plains, at least at the resolution of most global images. In addition, changing surface patterns can confuse attempts to correlate left and right stereo images, and radiation noise in Galileo images can complicate mapping.

We have mosaicked 70 stereo DTMs derived from Voyager and Galileo imagery (controlled using the Galileo limb profiles) to create a topographic map covering ~75% of Io in order to constrain the shapes of regional- and global-scale features on this volcanic moon. This abstract discusses how we have used this map, in conjunction with other datasets, to investigate the variation of heat flow across the planet and its relation to tidal heating mechanisms [6].

Methods: Customized ISIS software at LPI has been used to create and process stereo DTMs of Io's surface using Voyager and Galileo imagery. The stereo routine determines parallax and associated topographic relief by identifying corresponding pixels within the two stereo images through matching albedo patterns in finite-sized patches. Where the surface is smooth and featureless, the inability of the program to identify corresponding pixels can contribute to noise in the data, which must be masked automatically or manually. We have refined the stereo mapping technique described in previous research [7,8] by varying the size of the patch depending on the apparent relief of the terrain as determined from observing the parallax between the left- and right-hand stereo images. Low relief areas such as the plains are processed with large patch sizes, which smoothens the resulting DTM and reduces noise, while high relief areas such as mountains and layered plains are processed with small patch sizes, which retains fine details in the topographic signatures of these features. Separate DTMs created using different patch sizes are then mosaicked together.

Whenever possible, we control the stereo DTMs in order that they fit the triaxial ellipsoid of Io as defined by 25 Galileo limb profiles [5] before they are globally projected and mosaicked together. Of the 70 DTMs, 35 have been controlled using the limb profiles, and 32 have been controlled using overlapping, controlled DTMs.

Results: The final, controlled DTM is shown in Fig. 1. Its quality can be assessed by quantifying topographic residuals between profiles with identical ground tracks in the limb and DTM data. We find that the mean absolute residual has a magnitude of 0.61 km; 51.6% of all the residuals have a magnitude less than 0.5 km, while 19.5% have a magnitude of 1 km or greater. The long-wavelength topographic variation of Io is quantified by removing topography associated with high-relief features (e.g. mountains, layered plains and some paterae), such that only the smoothed relief in the interstitial plains areas between -2 and +2 km in elevation remains. The resulting global mean elevation is 0.00 km (σ = 0.61 km), and 89.9% of the elevation values for the plains areas are within ±1 km elevation, indicating minimal topographic variation across Io that is consistent with the magnitude of variation as determined by previous control point network and limb profile studies [9,5]. We do not observe the previously reported 90° spacing of longitudinal basins and swells [9] in our DTM, but we have identified an arrangement of basins and swells with a wavelength of ~130° of longitude, and an amplitude of 1 to 1.5 km, the boundaries of which (as far as can be determined in our DTM) are shown in Fig. 1.

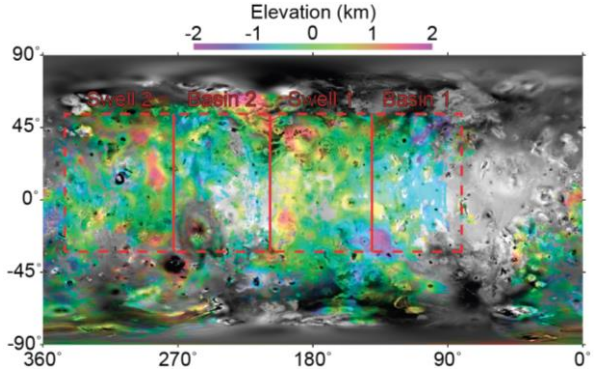

Fig. 1. Stereo DTM overlain on a mosaic of visible Voyager and Galileo images in simple cylindrical projection at 2 km/px. Gaps in the DTM represent masked noise or absence of stereo coverage. The boundaries of the basins and swells as identified in the DTM are indicated by red lines.

We have assessed the extent to which the long-wavelength topography in our stereo DEM can be correlated to the distribution of volcanoes and mountains. Independent studies [10,11,12] have identified bimodal, equator-centered peaks in volcano and mountain distributions that are anticorrelated, i.e. offset by 90° to each other. These correspond reasonably well to the locations of the basins and swells identified in our DTM, with the caveat that the boundaries of these features are not well defined due to limitations in stereo coverage. The statistics in Table 1 indicate the correlation of our swells and basins to regions with high spatial densities of volcanoes and mountains, respectively. Fig. 2 maps the locations of the peaks in mountain/volcano distribution [11], with the locations of our basins and swells overlain.

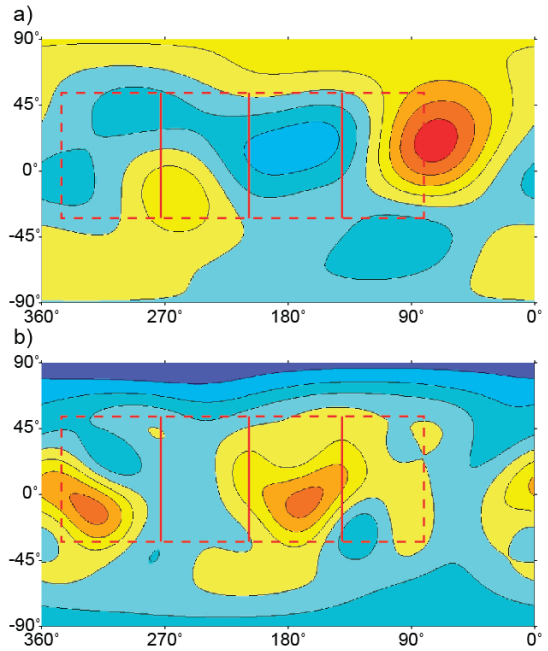

Fig. 2. Map of the spatial distribution of mountains (a) and volcanoes (b) [11]. High densities are in red, low densities are in blue.

Implications for heating: How heat is transferred from Io's interior to its surface, and the location of the primary source of the tidal heating, are considered to be instrumental in governing the distribution of mountains and volcanoes. A plausible scenario involves mantle or asthenospheric convection acting to offset the global crustal compressive stress field induced by volcanic subsidence that is regarded to be responsible for mountain formation [10], thereby leading to enhanced volcanism and decreased mountain building in some areas. Modeling of convection in Io's interior [6] indicates that the location of tidal heating strongly influences internal dynamics and heat flow distribution, with an asthenospheric heating scenario predicting increased heat flow along the tidal axis, coincident with the swells and volcano concentrations, and decreased heat flow at the leading and trailing points on Io, coincident with the basins and mountain concentrations. The association of the swells with volcano concentrations supports the hypothesis that these areas are experiencing upwelling of asthenospheric material, creating a net extensional stress that promotes enhanced volcanism. This offsetting extensional stress will be reduced, if not absent, in the areas with lower surface heat flow where the basins coincide with mountain concentrations, and compressional stresses associated with burial, subsidence and compression of volcanic deposits predominate. In this sense, the basins and swells identified in our DTM would appear to support an asthenospheric tidal heating model for Io. Despite the incomplete stereo coverage, we therefore consider the correlation between the volcano/mountain concentrations and the basins/swells in our DTM to be significant with respect to refining scenarios for global heating on Io.

References: [1] Pike R.J. (1974) *Geophys. Res. Lett.*, *1*, 291-294. [2] Bonner W.J. and Schmall R.A. (1973) *U.S. Geol. Surv. Prof. Pap.*, *812-A*. [3] Cintala M.J. and Mouginis-Mark P.J. (1980) *Geophys. Res. Lett.*, *7*, 329-332. [4] Pike R.J. (1980) *Lunar Planet. Sci. XI*, 2159-2189. [5] Thomas P. et al. (1998) *Icarus*, *135*, 175-180. [6] Tackley P.J. et al. (2001) *Icarus*, *149*, 79-93. [7] Schenk P.M. et al. (1997) *Geophys. Res. Lett.*, *24*, 2467-2470. [8] Schenk P.M. et al. (2004) *Icarus*, *169*, 98-110. [9] Gaskell R.W. et al. (1988) *Geophys. Res. Lett.*, *15*, 581-584. [10] Schenk P.M. et al. (2001) *J. Geophys. Res.*, *106*, 33,201-33,222. [11] Kirchoff M.R. et al. (2011) *Earth Planet. Sci. Lett.*, *301*, 22–30. [12] Hamilton C.W. et al. (2013) *Earth Planet. Sci. Lett.*, *361*, 272–286.

Table 1. Statistics associated with the basins and swells identified within the stereo DTM. Values in curved parentheses are 95% (2σ) confidence limits. The spatial density units for mountains and volcanoes are arbitrary, with negative and positive values representing densities below and above the global mean, respectively.

Basin/ swell	Basin/swell longitudinal boundaries (°W)	Basin/swell center longitude (°W)	Mean elevation in DTM (km)	Spatial density of mountains within basin/swell [11]	Spatial density of volcanoes within basin/swell [11]
Basin 1	81.1 to 140.8	110.9	-0.47 (±1.10)	0.079 (±0.310)	0.024 (±0.147)
Swell 1	140.8 to 208.5	174.6	0.17 (±0.99)	-0.145 (±0.153)	0.138 (±0.201)
Basin 2	208.5 to 273.0	244.7	-0.13 (±1.01)	-0.025 (±0.215)	-0.023 (±0.116)
Swell 2	273.0 to 345.5	310.6	0.12 (±1.04)	-0.060 (±0.148)	0.040 (±0.295)